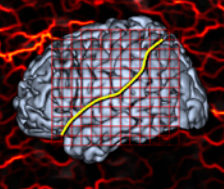




Local Adaptive Segmentation

Robert Dahnke, Gabriel Ziegler, Christian Gaser
Structural Brain Mapping Group, Department of Psychiatry
Friedrich-Schiller-University of Jena, Germany



INTRODUCTION

Segmentation of brain tissue into white matter (WM), gray matter (GM) and cerebrospinal fluid (CSF) is an important issue for studying cortical morphology and brain functions (Ashburner, 2005). After removing the noise and inhomogeneity, a Gaussian mixture model allows the tissue segmentation (Ashburner, 2000). However, even if the nonuniformity was removed completely, the tissue-contrast can be very poor. GM regions with high iron concentration, like the motor cortex and the occipital regions (Haacke, 2005), often have increased intensities that lead to misclassifications.

Here we present a new method that allows adaption of local intensity differences. Since these alterations happen relatively smooth within a tissue class, a region growing approach can be used to identify the segments more correctly. The extracted intensities afford corrections of the local image intensity.

METHODS

Input is a noise- and bias-corrected image (Figure 1a), and a brain mask (Dahnke et al., 2011). We start with clearly classifiable regions that are described by low gradients and class specific intensities that are estimated by a Gaussian mixture model (Figure 1b).

Then, a region growing that aligns voxel with similar intensity is used to dilate each class. A maximum distance and the specific intensities of other classes limit the region growing (Figure 1c). Nevertheless, it is possible that two classes align the same voxel. Because most neighborhoods contain class specific voxels, a small overlap is unproblematic and still allows a clear separation. We choose a 5x5x5 voxel box neighborhood.

After finding the major tissue segments, we can estimate the local intensity of each class voxel by averaging voxels of the same class within its neighborhood. To remove outliers only voxels within a SD below 80% of the maximum SD of the neighborhood are used.

As a result, each class voxel now contains the local intensity of its class (Figure 1d). To transfer these values to other non-class voxels, i.e. to get the GM value for a WM voxel, we estimate the hull of each class by morphological operations and set all outer voxels to the median class intensity. A Laplace filter with Dirichlet boundary condition is used to estimate the local intensity for all non-class voxels within the hull (Figure 1e). To avoid hard edges each class image is smoothed (Figure 1f). Finally, the input image T is scaled by the class maps, resulting in a map TSEG, with $WM=3$, $GM=2$, $CSF=1$, and $background=0$ (Figure 1g). After a second noise correction a CSF-GM-WM tissue segmentation with a MRF filter is used to create the final segmentation (Figure 2).

Calculation times with skull stripping, bias- and noise-correction take 4 minutes without, and 5 minutes with local adaption at 1 mm resolution.

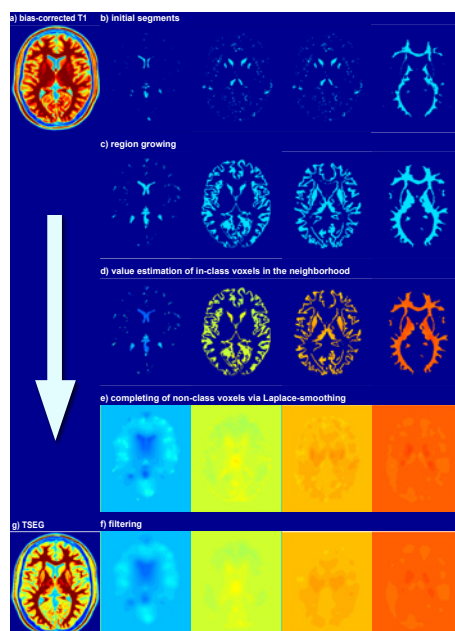


Figure 1: Main steps of the local adaptive segmentation algorithm. Initial segmentation and regions growing have the strongest influence on the final result. Overlapping of different tissue classes is possible (i.e. in subcortical structures), but unproblematic, if happens only for small areas. To control the smoothness of the results, the size of the neighborhood and the filter size are used (Figure 3). The intensity distance allows quantify the result of the segmentation (Figure 4).

RESULTS

For validation the Collins phantom (Collins et. al. 1998) with different noise level and inhomogeneity was used (Table 1). Because the phantom based on a segmentation and has thereby a good GM-WM contrast, the results are limited to test segmentation stability (Table 1). Besides this we used the IBSR2 dataset (<http://www.cma.mgh.harvard.edu/ibsr/>) to compare the method for more realistic conditions. Further single MR scans without ground truth segmentation were used for visual tests.

dataset	kappa(CSF)	Collins phantom	kappa(WM)	kappa(CSF)	IBSR2	kappa(WM)
method	0.7683±0.0326	0.8770±0.0471	0.9000±0.0465	0.0750±0.0422	0.7492±0.1321	0.8095±0.0985
SPM8	0.7487±0.0213	0.9172±0.0231	0.9392±0.0194	0.1283±0.0446	0.7870±0.0235	0.8571±0.0213
VBM8	0.7281±0.0507	0.8918±0.0618	0.9307±0.0469	0.1244±0.0461	0.7822±0.0238	0.8655±0.0259
our method	0.7491±0.0192	0.9014±0.0383	0.9362±0.0323	0.1387±0.0459	0.8328±0.0271	0.8330±0.0366

Table 1: Results of the segmentation of the Collins phantom with 0, 1, 3, 5, 7, 9% noise and 0, 20, 40, 80 % inhomogeneity, and real datasets of the IBSR2 database.

Preliminary results on real images indicate that the intensity scaling is able to improve the segmentation quality with lower representation of the GM in the motor cortex and a better representation of subcortical GM (Figure 2).

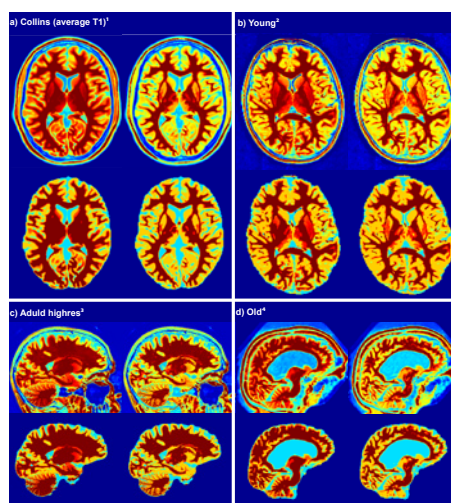


Figure 2: Results of our local adaptive segmentation for 4 persons (a-d). In each subfigure the top left images shows the original bias corrected image and its segmentation below, whereas the right side shows the intensity scaled version of the original on the top and its segmentation below. For all segment images (bottom of each subfigure) and the intensity scaled image (top left) the colors are coded in the following way: dark red is WM, yellow is GM, cyan is CSF, and dark blue is background.

Figure 3 shows the impact of the neighborhood and filter size. A small neighborhood and low smoothing lead to harder results, whereas higher values lead to smoother images with less local differences.

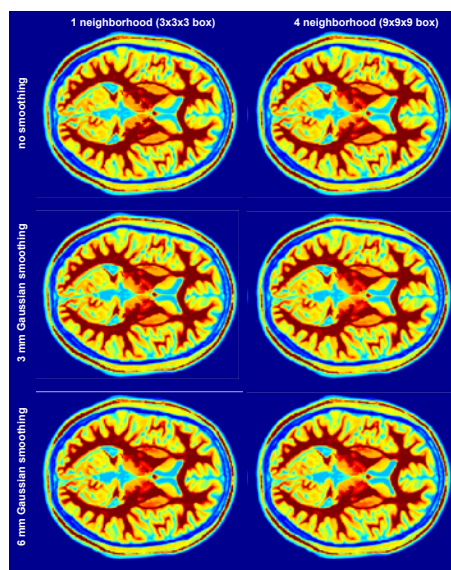


Figure 3: Besides the region initialization, and region-growing parameter, the size of the neighborhood for the class intensity estimation and the smoothing size influences the results. Small neighborhoods (left) and low smoothing (top) lead to very hard boundaries that strongly depend on the estimated segments. Higher neighborhoods and higher smoothing (bottom) reduces local sensitivity a little bit, but helps to increase the stability.

Furthermore, our method allows the description of local tissue contrast (Figure 4) that may be able to identify special regions or to quantify local segmentation quality. Higher segmentation errors are expected in regions with low contrast (red) and results have to be handled more carefully than for regions with good contrast (blue).

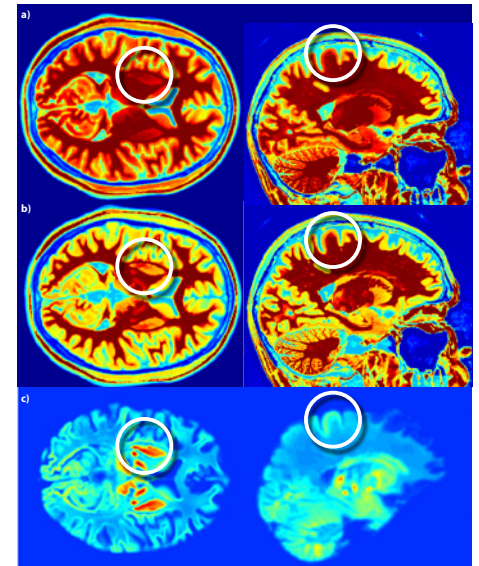


Figure 4: Shown are the original bias corrected image (a), the intensity corrected image (b) and the inverted contrast map (c) that describes the contrast between the estimated tissue classes. Higher segmentation errors are expected in regions with low contrast (red) and results have to be handled more carefully than for regions with good contrast (blue).

CONCLUSIONS

We have presented a new method that allows a local adaptive segmentation for varying tissue contrast and a way to appraise the quality of the segmentation based on the contrast between the tissue classes.

Another similar idea of local adaptive segmentation is presented on **poster 672** (Gaser et. al. 2012). Compared to the here described method, it use ROIs to locally equalize the histogram before segmentation.

Although both methods show visual improvements and good preliminary quantitative results for the Collins Phantom and IBSR database, further evaluation is necessary for a detailed understanding of the local changes of the PVE for the GM/CSF and GM/WM boundaries and depending measures like cortical thickness.

ACKNOWLEDGEMENTS

Robert Dahnke, Gabriel Ziegler, and Christian Gaser are supported by the German BMBF grants 01EV0709 & 01GW0740.

Data

- 1) <http://imaging.mrc-cbu.cam.ac.uk/imaging/MniTalairach>
- 2) http://fcon_1000.projects.nitrc.org/indi/adhd200/
- 3) <http://www.spl.harvard.edu/publications/item/view/2037>
- 4) <http://www.oasis-brains.org>
- 5) <http://www.cma.mgh.harvard.edu/ibsr/>

REFERENCES

- Dahnke, R. et al. (2011), 'Partitioning of the brain using graph-cut', HBM2011.
- Ashburner, J. (2000), 'Voxel-based morphometry-the methods', NeuroImage, 11(6 Pt 1), 805-821.
- Ashburner et al. (2005), 'Unified segmentation', Neuroimage vol. 26 (3) pp. 839-851.
- Collins, D.L. et al. (1998), 'Design and construction of a realistic brain phantom', IEEE trans Med Imaging 17, 463-468.
- Gaser et al. (2012), 'Local Histogram Equalization to Improve Segmentation Quality of Low Contrast Structures', HBM 2012
- Haacke et al. (2005), 'Imaging iron stores in the brain using magnetic resonance imaging', Magnetic Resonance Imaging Volume 23, Issue 1, January 2005, Pages 1-25.
- Halle M, Talos I-F, Jakob M, Farouq S, Meier D, Wald L, Fischl B, Kikinis R (2011). Multi-modality MRI-based Atlas of the Brain.